Removal of Oxygen and Nitrogen from Niobium by External Gettering

Yong Hwan Kim*, Ryosuke O.Suzuki, Hiroshi Numakura**,
Hirobumi Wada** and Katsutoshi Ono

Department of Energy Science and Technology, Kyoto University
Yoshida-Honmachi, Sakyo-ku, Kyoto 606-01 Japan

Keywords

External Gettering, Purification of Niobium, Thermodynamics of Impurities, Oxygen Diffusion, Purity Estimation.

Abstract

External gettering has a potential to remove interstitial gaseous impurities from solid niobium even below 1500K. The oxygen concentration in the deposit and the Nb bulk is evaluated by a combination of material thermodynamics and mass balance. The removal of oxygen and nitrogen was experimentally studied by using Ti, Y, Zr, Al and Si. Titanium deposited smoothly on the Nb surface in vacuum, and absorbed the gaseous impurities most efficiently. By applying Ti as an external getter on commercial niobium at 1463K, the residual resistivity ratio (RRR) reached 780. The oxygen distribution was calculated by combining thermodynamics and diffusion data. The experimental deoxidation rate was found to be slower than the calculated value. This may be attributed to the slow growth of the deposited layer, its morphology, and the interdiffused Ti-Nb alloy layer.

---

* *Present address:* Pohang Iron & Steel Corp. Ltd., Nam-ku, Pohang, Kyungbuk, 790-785 Korea.

** Department of Materials Science and Technology, Kyoto University.

Introduction

Niobium is a promising r.f. superconductor for applications in quantum physics[1,2], where a good ductility and high thermal conductivity of thin sheet are required. Because the mechanical and physical properties of niobium are sensitive to the interstitial impurities, the removal of these impurities such as oxygen and nitrogen is essential[3-6].

Electron beam (EB) melting can remove the gaseous and volatile impurities from the molten Nb. The practical purity level after EB refining is, however, limited to a few tens mass ppm oxygen[7-9]. For further elimination, the ultra high vacuum (UHV) annealing over 2600K has been used in laboratory scale[3-6].

Another purification technique for Nb thin sheet is a solid state external gettering: the vapor of active metals such as Ti deposits on the Nb surface and this deoxidizes from the bulk[1, 10-12]. This method can be applied even below 1500K because the getter metals can establish an oxygen or nitrogen partial pressure much lower than that at UHV annealing. Its merits are, therefore, that it needs neither the higher vacuum system nor the higher temperature. For example, the Nb r.f. superconducting vessel 'cavity', which is contaminated by oxygen and nitrogen during the cold deformations and welding, could be purified even after its construction[1,2]. Peterson *et al.* reported in the deoxidation from vanadium that the key of this technique was the selection of reactive getter metals and the fast diffusion of gaseous elements in the matrix[13,14]. The oxygen diffusion in Nb was thought to be high enough to remove oxygen to the surface[1]. Concerning the selection of gettering metals, titanium was mainly chosen without clear thermodynamic consideration [1,2,10,11].

This work describes the thermodynamic basis of gettering mechanism and the selection of gettering metals available for Nb. The lowest limit of deoxidation by the external gettering is predicted, using the reported thermodynamic data. Keeping in mind that the combination of EB refining with external gettering may have a

potential for practical application, we studied experimentally the external gettering of the niobium pre-refined by EB.

Thermodynamics of External Gettering

1) Vapor pressure

Below 1500K, the oxygen partial pressure, p_{O_2}, in a Nb-10ppm O alloy is so low (for example, 1.41 x 10^{-21} Pa at 1463K[15]) that the oxygen atoms in this alloy can hardly evaporate into the gaseous phase. On the other hand, the selected getter metals, Ti, Y, Zr, Al and Si, have a higher vapor pressure than Nb, as shown in Table 1[16]. These metals will thus evaporate preferentially and deposit on the Nb surface, when they coexist with Nb in a sealed vessel at an elevated temperature.

2) With oxide and nitride of gettering metal

The getter solid metals are also selected from the common metals having a strong affinity with both oxygen and nitrogen. The partial pressure, p_{O_2}(eq:M-MO) and p_{N_2}(eq:M-MN) in the equilibrium between the getter metals (M) and their oxide (MO) and nitride (MN), respectively, are listed in Table 1[16]. In case that the getter metal is in equilibrium both with its oxide and with Nb-O alloy simultaneously (see case A in Fig. 1), p_{O_2} in Nb-O alloy is equal to p_{O_2}(eq:M-MO). The equilibrium oxygen concentration C_O(eq:M-MO) can be evaluated using the reported thermodynamic relationship between oxygen concentration C_O and p_{O_2} for Nb-O alloy[15],

$$\log_{10} C_O = -2.174 + 1/2 \log_{10} p_{O_2} + 19970/T \,, \qquad (1)$$

where C_O is in mass ppm, p_{O_2} in Pa and T in K. C_N(eq:M-MN) was similarly evaluated using Nb-N data[17], and is shown in Table 1. The temperature dependence of C_O(eq:M-MO) and C_N(eq:M-MN) is shown in Fig. 2 for titanium.

Titanium can deoxidize the Nb-dilute oxygen alloy more strongly at the lower temperatures.

Judging from the above mentioned thermodynamic consideration, yttrium is the most desirable deoxidizing metal among the selected ones: It has a potential to remove oxygen to 0.20 mass ppb at 1463K. Due to the weak affinity of Y with nitrogen, however, C_N(eq:Y-YN) is as high as 270 mass ppm (see Table 1).

3) With the solid solution of gettering metal

Note that C_O(eq:M-MO) and C_N(eq:M-MN) correspond to the upper limits of purification when the getter metals exist as the metallic form. Without any precipitation of their oxide and nitride, the pure getter metals can remove the impurities more effectively by remaining in the getter metal-oxygen and -nitrogen solid solutions (see case B in Fig. 1). When this gettering mechanism works, for example, in case of thick deposition, the attainable impurity content can be lower than C_O(eq:M-MO) and C_N(eq:M-MN).

Consider that the Ti layer has existed on the Nb-O alloy before the annealing, and that this Ti layer absorbs oxygen from the Nb bulk during the annealing. Then, there exists $(V \cdot d_{Nb}/M_{Nb}) \cdot (M_{Nb}/M_O \cdot C_O(\text{initial in Nb})\ /10^6)$ mole oxygen in a volume V of Nb-dilute oxygen alloy, where d_{Nb}, M_{Nb}, M_O, and C_O(initial) are density of niobium, atomic weights of niobium and oxygen, and the initial oxygen content in mass ppm, respectively. Let the thickness of the Nb plate be a(in mm), and let the Ti thickness be b(in μm) on both sides of Nb, then the mass balance of oxygen before and after reaching the equilibrium is expressed as,

$$\left(\frac{10^3 \cdot a \cdot d_{Nb}}{M_{Nb}}\right) \cdot \left(\frac{M_{Nb} \cdot C_O(\text{initial in Nb})}{M_O \cdot 10^6}\right) + \left(\frac{2 \cdot b \cdot d_{Ti}}{M_{Ti}}\right) \cdot \left(\frac{M_{Ti} \cdot C_O(\text{initial in Ti})}{M_O \cdot 10^6}\right)$$

$$= \left(\frac{10^3 \cdot a \cdot d_{Nb}}{M_{Nb}}\right) \cdot \left(\frac{M_{Nb} \cdot C_O(\text{eq. in Nb})}{M_O \cdot 10^6}\right) + \left(\frac{2 \cdot b \cdot d_{Ti}}{M_{Ti}}\right) \cdot \left(\frac{M_{Ti} \cdot C_O(\text{eq. in Ti})}{M_O \cdot 10^6}\right) \quad (2)$$

where C_O(eq. in Nb) and C_O(eq. in Ti) are the equilibrium oxygen content in metallic Nb and that in metallic Ti, respectively.

In β-titanium-dilute oxygen solid solution, for example, the oxygen partial pressure p_{O_2} is given as[18]

$$\log_{10} C_O(\text{in } \beta\text{-Ti}) = -3.106 + 1/2 \log_{10} p_{O_2} + 30440/T \, . \quad (3)$$

By combining this equation with eq.(1), the equilibrium oxygen content becomes

$$\log_{10}\{C_O(\text{eq. in Nb}) / C_O(\text{eq. in } \beta\text{-Ti})\} = 0.933 - 10470/T \, . \quad (4)$$

Assuming that the initial oxygen content in Ti is null because oxygen in the commercial Ti can not be transferred to the Nb surface through the gaseous phase, we can deduce the oxygen content after the external gettering using eqs.(2) and (4). The results at 1463K are shown in Fig. 3. In the range of α-Ti, the reported thermochemical data[19] were assessed to adjust to the recent data of TiO[16]. Fig.3 indicates, for example, that the initial niobium containing 100 ppm oxygen changes to 0.63 ppb oxygen-Nb alloy by 100 μm Ti coating. The attainable oxygen concentration in Nb depends both on the thickness of the deposited Ti layer and the initial oxygen concentration in Nb. Because titanium exhibits a wide solubility range against both oxygen and nitrogen, it is one of the promising gettering materials.

Experimental

A. External gettering

A commercial Nb powder (1500 mass ppm oxygen, 700 ppm Ta, 22 ppm Fe, 20 ppm W, 4 ppm Al, <10 ppm Sn, <3 ppm Ni, Co, Mn, and Cr) was used as a starting material. The compacted powder was repeatedly melted on water-cooled copper plate by 31.5 kW electron beam[8,9]. About 100g Nb buttons obtained were cold-drawn into the wire of 1.4 mm in diameter, or 1.0 mm thick plate, without intermediate annealing. For electric resistivity measurement, 150 mm long wire was

coiled into a 45 mm long spring. The contaminated surface of the specimen was etched by the HF aqueous solution.

The Nb specimens were wrapped with the foil of pure Ti, Y, Zr or Al thinner than 0.1 mm. Only in case of Si, high purity Si powder was used instead of its foil. The wrapped samples were heated in an evacuated quartz tube with getter metal blocks. Because thermodynamically these getter metals can reduce SiO_2, the quartz tubes were damaged by the metallic vapor. Even after 72 hours at 1463K, however, the ampoule maintained its shape without leakage. The coated film of getter metal was removed by the HF solution if necessary.

B. Purity Evaluation

The content of oxygen and nitrogen in the samples was analyzed by an inert gas fusion-infrared absorption method using LECO TC-336. Because the oxygen and nitrogen in the Pt extraction bath are counted together with those in Nb samples, the analytical value includes the deviation of $\pm$20 mass ppm oxygen and of $\pm$5 mass ppm nitrogen. Both the starting wires and the plates were, therefore, analyzed as 60$\pm$ 20 ppm oxygen and 25$\pm$5 ppm nitrogen after EB refining.

Because the impurity content in the purified Nb fell below the lowest detection limit of conventional gas analysis, we needed an alternative measure, which could be also available for complex shape such as cavity. At a single ppm impurity level,a handy gauge can be obtained by the electrical resistivity $\rho(T)$ [3-6, 20,21].

The electrical resistivity $\rho(T)$ at temperature T is expressed for pure metals by Matthiessen's rule. By a sufficiently long annealing of a sufficiently thick sample, $\rho(T)$ changes with impurity content, C_i, according to;

$$\rho(T) = \rho_{\text{intrinsic}}(T) + \sum_{\text{impurity}} \alpha_i C_i \quad . \tag{5}$$

The resistance $R(T)$ is expressed by $\rho(T)$ and the size factor k,

$$k \equiv l / A \, , \tag{6}$$

where l and A are the distance between potential leads and the cross-sectional area of the sample, respectively. Then,

$$k \equiv \frac{R(T)}{\rho(T)} = \frac{R(273\mathrm{K})}{\rho(273\mathrm{K})} = \frac{R(77\mathrm{K})}{\rho(77\mathrm{K})} = \frac{R(273\mathrm{K}) - R(77\mathrm{K})}{\rho(273\mathrm{K}) - \rho(77\mathrm{K})} \quad . \quad (7)$$

Abraham and Devoit[20] reported that the difference ρ(273K)-ρ(77K) was commonly 1.0881 x 10^{-7} Ωm for any grade of pure niobium. The definition given by the last term of eq.(7)[20,21] is convenient for the coiled samples. The size factor k thus defined was well coincident with the value k measured following eq.(6) within our experimental accuracy of l and A.

$R(T)$ of the sample was measured by the standard four probe method with 0.01 μΩ in accuracy, using ice water, liquid N_2 and liquid He. To quench the superconductivity of Nb at 4.2 K, the external magnetic field was applied up to 17 kOe. Their superconductivity were completely broken at least by 5 kOe. ρ(4.2K) at 0Oe was evaluated by extrapolating from the normal conducting region in the higher magnetic field because the resistivity induced magnetically was overlapped.

Oxygen and nitrogen in solid solution give rise to separate Snoek peaks, whose heights are proportional to the concentration of the respective solute[22,23]. Internal friction measurements were made on wire specimens of 50mm long using a conventional inverted torsion pendulum apparatus[24]. Internal friction, Q^{-1}, was measured by the free-decay method with increasing temperature at the rate of 1 K/min under a helium atmosphere of 50 Pa. The oscillation frequency was in the range between 0.75 and 0.85 Hz.

Results and Discussion

A. External gettering

Fig. 4 shows the cross-section of the Nb sample annealed with Ti at 1373K for 18 hours. Ti deposit covered the whole surface smoothly, and its layer thickness was 5μm at 1073K for 18hours. The Ti layer became thicker as the isochronal

annealing temperature increased, and it reached 265 μm at 1463K. A concentration profile by EDX in Fig. 4 shows that niobium diffused out to the Ti deposited layer, but that the penetration of Ti into the Nb substrate was limited to a few tens μm. This reaction zone as well as the coated film could be easily removed by chemical etching.

Fig. 5 shows the cross-sectional views of the samples annealed with the other getter metals at 1373K for 18hours. Zirconium could not coat the Nb surface smoothly; A few spotty Zr deposits were formed especially at the points contacting mechanically with Zr foil. This is because the Zr vapor pressure is the lowest among the selected metals listed in Table 1. Yttrium covered the whole Nb surface, but its thickness was a tenth thinner than that of the Ti layer after the same heat treatment. Padamsee reported that Y coated sufficiently thick in a few hours at 1523K[12]. This discrepancy may be attributed to the waste of getter metal vapor to the vacuum vessel. Yttrium attacked heavily the quartz ampoule, and some trials using Mo foils failed to separate Y vapor from the ampoule. The contamination by Si due to the reduction of SiO_2 was often detected in Y layer. In case of silicon, the Si deposit formed an irregular layer thinner than 1 μm in the examined temperature range of 1073K to 1463K. Aluminum formed the granular $NbAl_3$ grains on the Nb samples. The deposited layer for all the studied samples contained neither oxide nor nitride, based on X-ray diffraction measurements.

B. Electrical Resistivity

The electrical resistivity is a good measure to evaluated the purity, but some scatters are found among the previous reports[3-6,20,21,23] probably because of the metallic impurities. To evaluate the oxygen dependency of the electrical resistivity in our samples, 1 mm thick Nb sheets were cut off from the ingots, which had been oxygen-doped and weakly refined in the EB furnace[8,9]. The homogeneous distribution of impurities had been checked by micro-hardness measurements[8,9]. The relationship between the electrical resistivity and the oxygen concentration

shows a good linearity at the high oxygen concentration range over 100mass ppm as shown in Fig. 6, assuming the contribution to the resistivity by small amount of nitrogen (<20 mass ppm) is nearly the same as the oxygen contribution[4]. The proportionality factor α in eq.(1) is calculated to be 4.81(±0.02) x 10^{-12} Ωm/at.ppm (oxygen+nitrogen), which agrees well with the previous reports compiled by Schulze et al.[4]. The extrapolation to zero impurity 1.313(±0.008) x 10^{-7} Ωm is slightly smaller than the previous values(1.325-1.343 x 10^{-7} Ωm)[4]. This linear regression is used as a measure of purity for our samples.

The starting wires used for the external gettering contain heavy deformation due to the cold drawing, and their ρ(273K) were scattered from 1.354 to 1.345 x 10^{-7} Ωm. After independent vacuum annealing with Nb foil, ρ(273K) approached about 1.344 x 10^{-7} Ωm, which agreed with ρ(273K) (≅1.343 x 10^{-7} Ωm) for the Nb sheet cut off from the EB ingot used for drawing.

The resistivities of the samples gettered at 1373K for 18 hours were measured in coil shape after careful removal of the deposited film. ρ(273K) is listed in Table 2. Y, Si and Al, as the getter metals, did not decrease the resistivity significantly. It is due to their thin deposited layers and their morphology as shown in Fig.5.

Fig. 7 and 8 show the electrical resistivity and Vickers' microhardness, respectively, after the external gettering with Ti or Zr. For all the annealed samples, the conventional gas analysis showed a value below the lower limit of quantitative analysis (<70 mass ppm oxygen and <15 mass ppm nitrogen). By rising the isochronal annealing temperature, both ρ(273K) and hardness decreased. These decreases indicate that the higher purity can be obtained at the higher temperatures, and they are opposite to the temperature dependence of C_O(eq:M-MO) as shown in Fig. 2. This comparison shows the importance of kinetic factors, which will be discussed later.

ρ(273K) and hardness of the Nb samples annealed with Zr are higher than those annealed with Ti. Considering the similar thermodynamic properties of Ti and Zr as listed in Table 1, this is due to the spotty deposits of Zr. It shows the purification depends on the deposited layer's thickness and its morphology.

The electrical resistivity ρ(273K) is shown in Fig. 9 for the samples annealed with Ti isothermally at 1463K. The significant drop of ρ(273K) occurred within a day. Because the effect of plastic deformation can be wiped out in a hour, the successive decrease in ρ(273K) is due to deoxidation and denitrization. The impurity scale in Fig. 7 and 9 are extrapolated from the region higher than 100 mass ppm shown in Fig. 6. Some values of ρ(273K) fall below the zero impurity level in this scale. This is attributed to the scatter of data over 100 ppm and the linear regression analysis, but this scale indicates the sequence of purification by the external gettering.

The residual resistivity ratio (RRR) is here defined as ρ(273K)/ρ(4.2K). RRR for some gettered samples shown in Fig. 9 are calculated directly as R(273K)/R(4.2K). Fig. 10 shows RRR for the sample annealed with Ti at 1463K. The highest RRR (=780) was recorded for the sample annealed for 42 hours.

C. Internal friction

Figure 11 shows the internal friction profiles of the specimen annealed without titanium (A) and with titanium (B). The two peaks in the former, one at 422K and the other at 560K, are the Snoek peaks of oxygen and nitrogen, respectively. For a randomly oriented polycrystalline niobium specimen, the peak height per atomic percent solute is reported to be 4.5×10^{-2} for oxygen and 5.0×10^{-2} for nitrogen[22]. Then C_O and C_N in this specimen (A) are evaluated to be 86 and 53mass ppm, respectively.

Since the used wire specimen was prepared by cold-drawing, it might retain the <110> fiber texture, which is common to the BCC metals[25], even after the

annealing. If this is the case, a correction is necessary for the proportionality constant because of the dependence of the peak height on crystal orientation. Because the correction factor for <110> orientation is 1.33[24], C_O and C_N are evaluated as 65 and 40mass ppm, respectively, which are reasonably close to those determined by chemical analyses.

In contrast, the Snoek peaks were barely detected for the specimen (B) annealed with Ti at 1463K for 42hours(curve B). This demonstrates that the amounts of residual oxygen and nitrogen were reduced to single mass ppm level by the external gettering.

Considering that our commercial niobium contains 700ppm Ta, the further improvement of RRR can be achieved by removing such metallic impurities. Note that hydrogen as a possible impurity is not considered here. A prolonged annealing may cause the contamination from the gettering metal and the quartz ampoule.

D. Kinetics

The purification of Nb bulk should obey the second thermodynamic mechanism proposed as case B in Fig. 1, because all the deposited layer were found to be metallic. The temperature dependency of the impurity level (Fig. 9 and 10) indicates, however, that the kinetics of deoxidation plays a dominant role for the external gettering mechanism.

The oxygen distribution was calculated numerically from Fick's law, assuming the unidirectional diffusion of oxygen from 1 mm thick Nb to 100 μm thick Ti. Fig.12 demonstrates the change of oxygen profiles at 1463K. The initial 100 mass ppm oxygen in Nb diffuses into Ti layer, keeping the local equilibrium (eq.(4)) at the interface. Because the diffusion coefficient of oxygen in β-Ti is similar with that in Nb[26,27], the oxygen inflow into Ti can spread out quickly. At 1463K the equilibrium distribution is completed in a few hours.

By integrating the oxygen profile in Nb, the average oxygen concentration is evaluated in Fig.13. Below 1300K, the equilibrium can not be reached in the practical period. Especially the deoxidation hardly occurs below 1155K, because the oxygen diffusion in α-Ti is 1/100 slower than that in β-Ti. Note also that nitrogen diffusion is a few times slower than oxygen diffusion[26,27].

The mutual diffusion of metallic elements in the coated layer is essential for the external gettering; Once the deposited Ti makes an alloy with Nb, the back evaporation from deposited layer is suppressed, and the layer thickness increases with gettering time. This Ti-Nb alloy layer may be unable to absorb oxygen and nitrogen as effective as the pure Ti layer. Both the thermodynamic data and diffusion data in this alloy layer may be useful for further analysis.

An homogenous thickness of Ti deposit was assumed for calculation, but in the experiments we found that the Ti layer grew up continuously during the isothermal annealing. Further improvement of modeling will be needed.

Conclusions

Niobium was purified by a combination of electron beam melting and external gettering. The purity was characterized by measurements of the electrical resistivity and internal friction. A Nb sample gettered by Ti at 1463K barely shows Snoek peaks due to oxygen and nitrogen, and RRR exceeded 500.

From a thermodynamic point of view, Y and Zr are known as effective deoxidizing metals. Two models are analyzed: The first is the case that the getter metals coexist with their oxide and/or nitride, and the second is the case that they form a dilute alloy with oxygen and/or nitrogen. In equilibrium of the latter case, the deoxidation to a sub ppm level is possible, even if Ti is used. The morphology and the thickness of the gettering metal layer on the Nb surface, however, affected more strongly the deoxidation and denitrogenation. The mutual diffusion of Nb and Ti may also prevent achieving the thermodynamic equilibrium state.

Acknowledgments

The authors thank Mr. Isao Nishikawa and Mr. Masayuki Aizawa for their experimental assistance, and Mr. M. Unezaki for EPMA analysis. Kim would like to express his gratitude to Prof. Young Hyun Paik, Korea University, for his encouragement and to Park Yong Ku Scholarship Foundation in Tokyo.

References

1 P. Kneisel, *J. Less-Common. Met., 139* (1988) 179.

2 H.Padamsee, *J. Less-Common. Met., 139* (1988) 167.

3 R.W.Meyerhoff, *J.Electrochem.Soc., 118* (1971) 997.

4 K.Schulze, J.Fuss, H.Schultz and S.Hofmann, *Z.Metallk., 67* (1976) 737.

5 K.Schulze, E. Grallath and M.Weller, *Z.Metallk., 72* (1981) 439.

6 K.Schulze, *J. of Met., May* (1981) 33.

7 K.Ono and Y.H.Kim, *ISIJ International, 30* (1992) 650.

8 Y.H.Kim, T.F.Kumon and K.Ono, *Proc. 1st Int. Conf. on Processing Materials for Properties*, TMS, Ohio, 1993, p.943.

9 K.Ono, Y.H.Kim, T.F.Kumon, T.H.Okabe and R.O.Suzuki, *Proc. Klaus Schulze Symp. on Processing and Applications of High Purity Refractory Metals and Alloys*, TMS, Ohio, 1994, p.179.

10 R. Kirchheim, *Acta Metall., 27* (1979) 869.

11 O.Yoshinari, T.Konno, K.Suma and M.Koiwa, *J. Less-Common Met., 81* (1981) 239.

12 H.Padamsee, *IEEE Trans. Magn., MAG-21 No.2* (1985) 1007.

13 D.T.Peterson, R.G.Clark and W.A.Stensland, *J. Less-Common Met., 30* (1973) 169.

14 D.T.Peterson, B.A.Loomis and H.H.Baker, *Metall.Trans.A, 12A* (1981) 1127.

15 W.Nickerson and C.Alstetter, *Scr. Metall., 7* (1973) 229.

16 A.Roine, *Outokumpu HSC Chemistry for Windows, Ver.2.03,* Outokumpu Research Oy, Pori, Finland, 1994.

17 E.Gebhardt, E.Fromm and D.Jakob; *Z.Metallk., 55* (1964) 423.

18 T.H.Okabe, R.O.Suzuki, T.Oishi and K.Ono; *Mater. Trans., JIM., 32* (1991) 485.

19 O. Kubaschewski and W.A.Dench; *J.Inst.Metals, 82* (1953-54) 87.

20 J.M.Abraham and B.Deviot, *J. Less-Common Met., 29* (1972) 311.

21 D.G.Westlake, *J. Less-Common Met., 33* (1973) 391.

22 A. S. Nowick and B. S. Berry, *Anelastic Relaxation in Crystalline Solids,* Academic Press, New York, 1972, p.225.

23 E.Gebhardt, R.Rothenbacher, *Z.Metallk., 54* (1963) 443.

24 H. Numakura, M. Miura, H. Matsumoto and M. Koiwa, *ISIJ International, 36* (1996) 290.

25 C. Barrett and T. B. Massalski: *Structure of Metals*, 3rd edn, Pergamon, Oxford, 1980, p. 545.

26 G. Hoerz, H.Speck, E.Fromm and H.Jehn, *Physik Daten, Gases and Carbon in Metals, Part.VIII: Group VA Metals (2) Niobium,* Energie Physik Mathematik GmbH, Karlsruhe, 1981, p.24.

27 H.Jehn, H.Speck, E.Fromm and G. Hoerz, *Physik Daten, Gases and Carbon in Metals, Part.V: Group IVA Metals (1) Titanium,* Energie Physik Mathematik GmbH, Karlsruhe, 1979, p.14.

Table Captions

Table 1 Thermodynamic data at 1463K for the getter metals.

Table 2 Resistivity ρ(273K) for Nb samples before and after the external gettering at 1373K for 18 hours. For each getter metal, two samples were measured. The resistivity before gettering contain the effect of cold working.

Figure Captions

Fig. 1 Thermodynamic models of the external gettering.

Fig. 2 Oxygen concentration in niobium in equilibrium with Ti and TiO, and nitrogen concentration in niobium in equilibrium with Ti and TiN.

Fig. 3 Calculated oxygen concentration in 1mm thick niobium plate, on whose surfaces the thin titanium layers are attached. The initial concentration C_O(initial in Nb) is reduced to C_O(eq. in Nb) after equilibrium at 1463K.

Fig. 4 Electron Probe Micro Analysis (EPMA) of the cross-section of the sample annealed with Ti foil at 1373K for 18 hours. The metallic concentrations were analyzed along the white line indicated in the photo.

Fig. 5 Cross-sectional views of the deposits on Nb samples, which were annealed with Zr, Y, Si and Al at 1373K for 18 hours.

Fig. 6 Relationship between the sum of oxygen and nitrogen concentration, and the electrical resistivity at 273K.

Fig. 7 Electrical resistivity at 273K of the samples annealed for 18 hours with Ti and Zr.

Fig. 8 Vickers' hardness of the samples annealed for 18 hours with Ti and Zr.

Fig. 9 Electrical resistivity at 273K of the samples annealed at 1463K with Ti.

Fig. 10 Residual resistivity ratio of the samples annealed at 1463K with Ti.

Fig. 11 Internal friction profiles of the sample (A) annealed without Ti, and of the sample (B) annealed with Ti, for 42 hours at 1463K.

Fig. 12 Calculated oxygen profiles at 1463K, where the surfaces of 1 mm thick niobium plate are coated by 100 □m thick titanium layers.

Fig. 13 Average oxygen concentration in 1mm thick niobium plate, whose surfaces are coated by 100 □m thick titanium layers. Oxygen distributions were calculated for two annealing times, 3 hours and 18 hours.

Table 1 Thermodynamic data at 1463K for the getter metals.

Element	Vapor Pressure	Equilibrium pressure with oxide †	Equilibrium pressure with nitride †	Equilibrium concentration in Nb[15,17]	
	$p_{Vap.}$ (Pa)	p_{O_2}(eq.M-MO) (Pa)	p_{N_2}(eq. M-MN) (Pa)	C_O(eq.M-MO) (mass ppm)	C_N(eq. M-MN) (mass ppm)
Nb	1.36×10^{-13}	(1.41×10^{-21})*	(1.76×10^{-9})**	-	-
Ti	4.16×10^{-5}	1.37×10^{-24}	5.36×10^{-10}	0.35	5.3
Zr	4.12×10^{-10}	4.25×10^{-25}	4.00×10^{-12}	0.20	0.45
Y	5.13×10^{-4}	4.34×10^{-31}	1.42×10^{-6}	2.0×10^{-4}	270
Al	7.15×10^{-1}	1.79×10^{-24}	5.87×10^{-7}	0.40	170
Si	4.33×10^{-4}	6.04×10^{-19}	2.32	230	***

†: Standard free energy of oxide or nitride was used[16].

*: p_{O_2} in the Nb-10mass ppm oxygen alloy[15]

**: p_{N_2} in the Nb-10mass ppm nitrogen alloy[17]

***: Nb can be fully nitridized to NbN by Si_3N_4.

Table 2 Resistivity ρ(273K) for Nb samples before and after the external gettering at 1373K for 18 hours. For each getter metal, two samples were measured. The resistivity before gettering contain the effect of cold working.

Getter metal	Before gettering	After gettering
(None)	-	≈13.44*
Ti	13.512 13.513	13.227 13.213
Zr	13.503 13.480	13.278 13.323
Y	13.542 13.472	13.332 13.471
Si	13.519 13.501	14.096 13.997
Al	13.462 13.458	13.501 13.460

* Average of 5 samples.

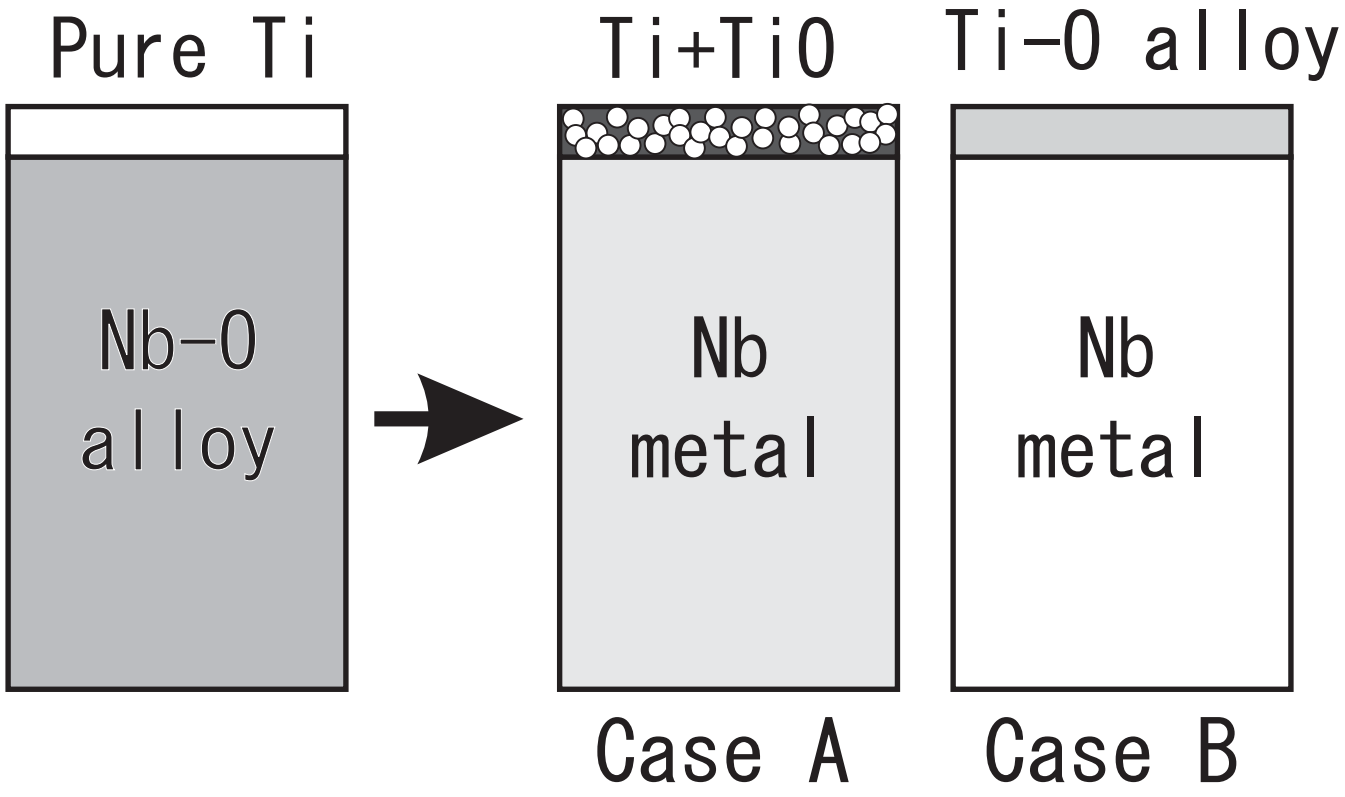

Fig. 1 Thermodynamic models of the external gettering.

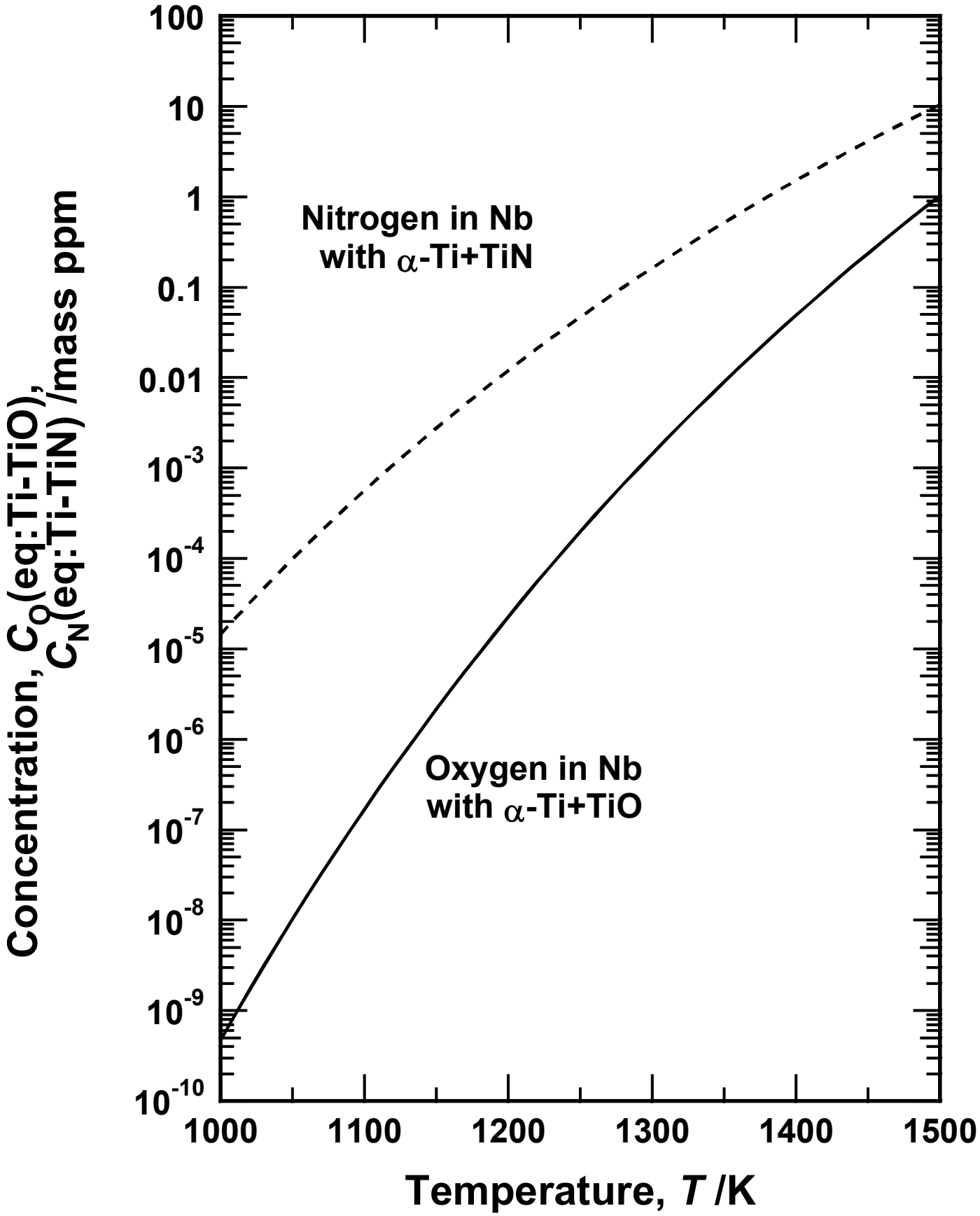
Concentration, C_O(eq:Ti-TiO), C_N(eq:Ti-TiN) /mass ppm
100
10
1
0.1
0.01
10^{-3}
10^{-4}
10^{-5}
10^{-6}
10^{-7}
10^{-8}
10^{-9}
10^{-10}
Nitrogen in Nb
with α-Ti+TiN
Oxygen in Nb
with α-Ti+TiO
1000
1100
1200
1300
1400
1500
Temperature, T /K

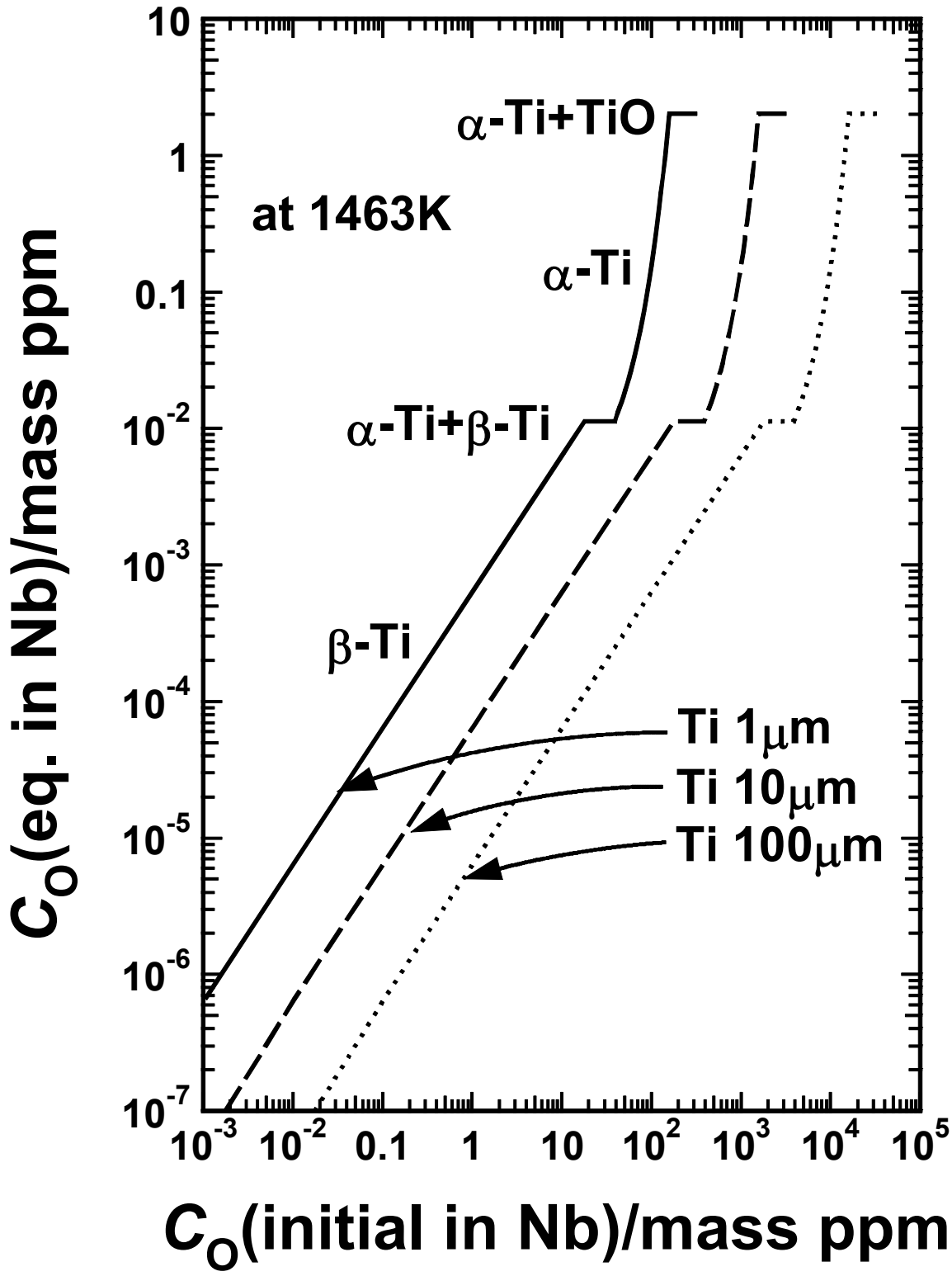

Fig. 3 Calculated oxygen concentration in 1mm thick niobium plate, on whose surfaces the thin titanium layers are attached. The initital concentration C_O(initial in Nb) is reduced to C_O(eq. in Nb) after equilibrium at 1463K.

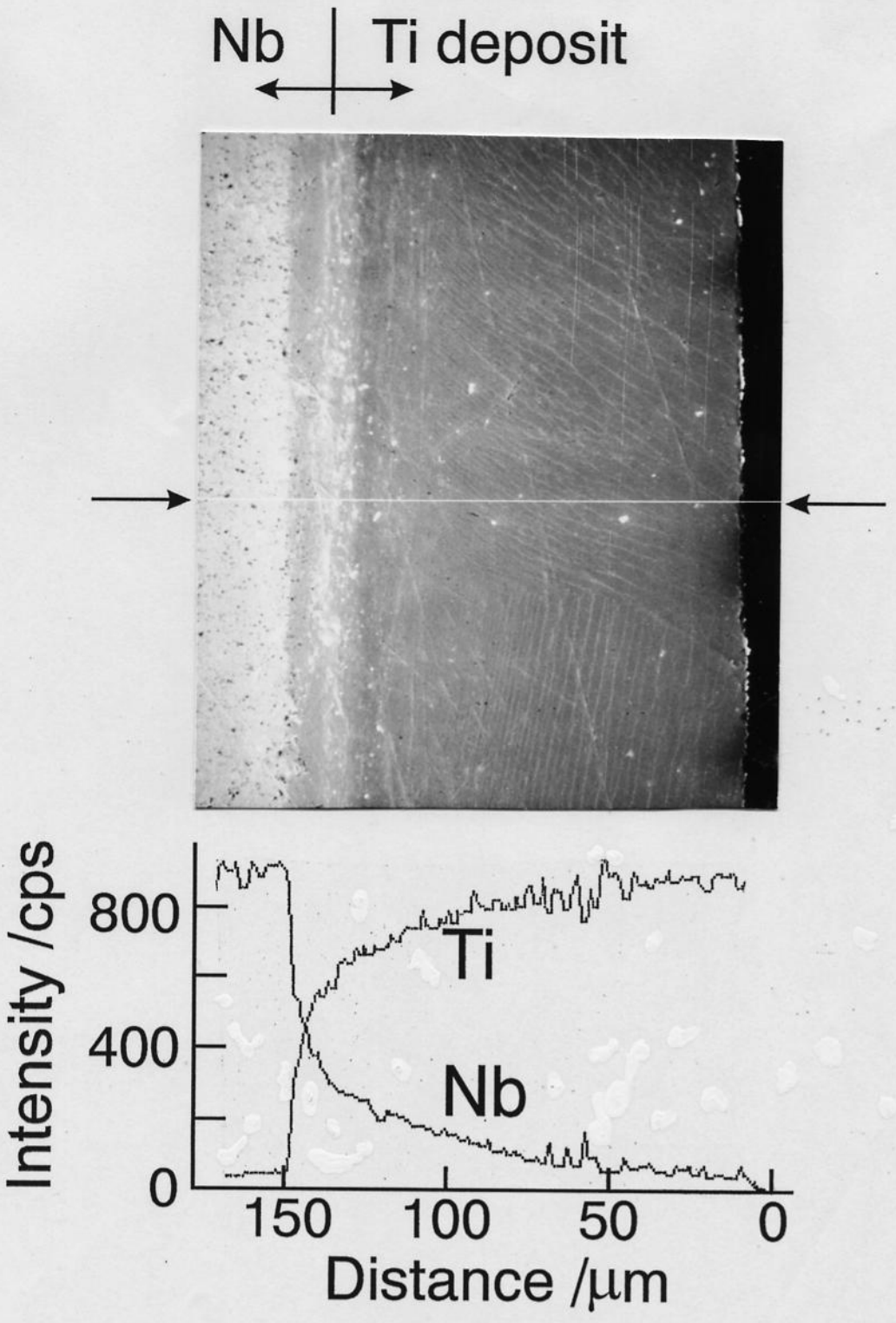
Nb
Ti deposit
Intensity /cps
800
400
0
Ti
Nb
150
100
50
0
Distance /μm

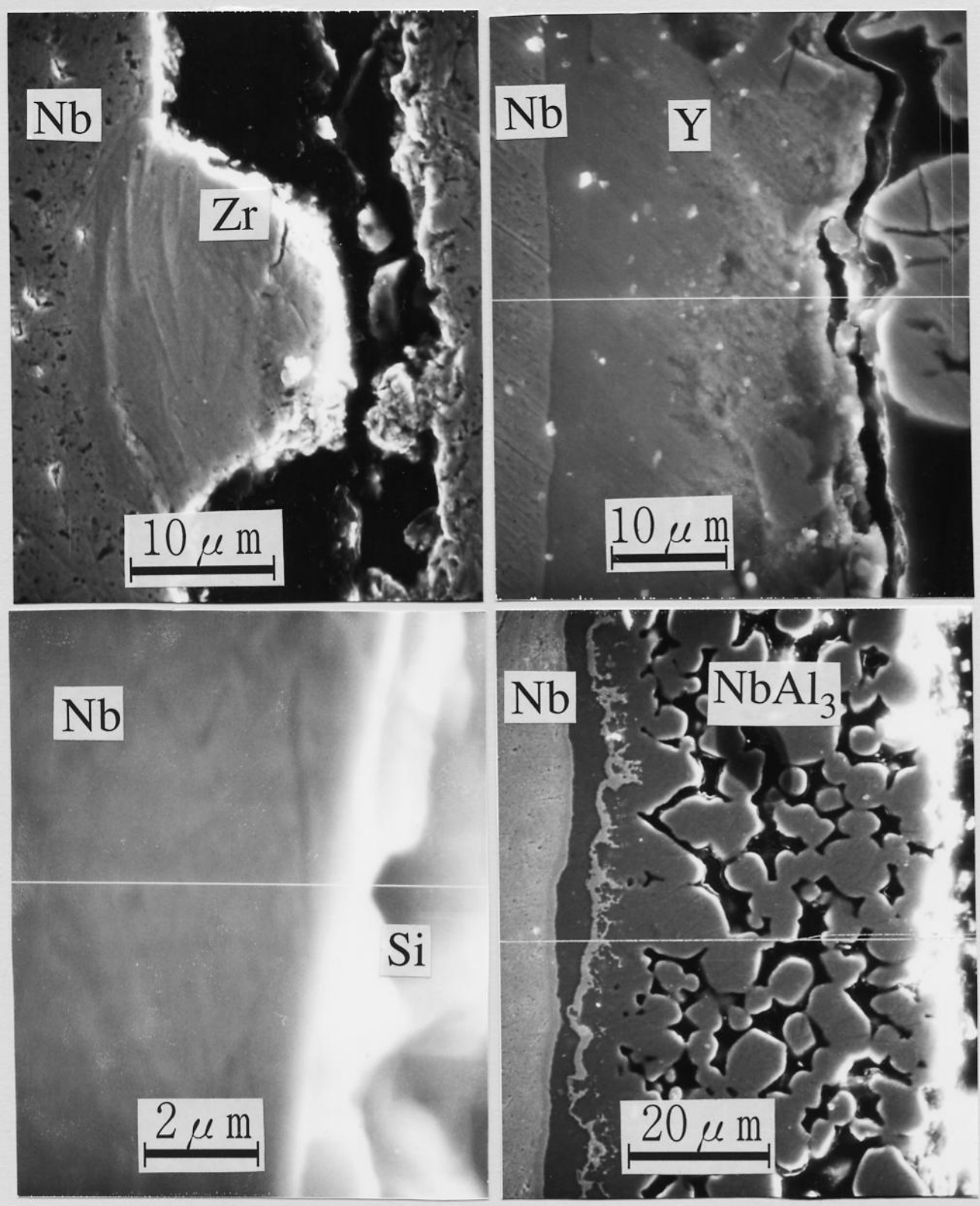
Nb
Zr
10 μm
Nb
Y
10 μm
Nb
Si
2 μm
Nb
NbAl3
20 μm

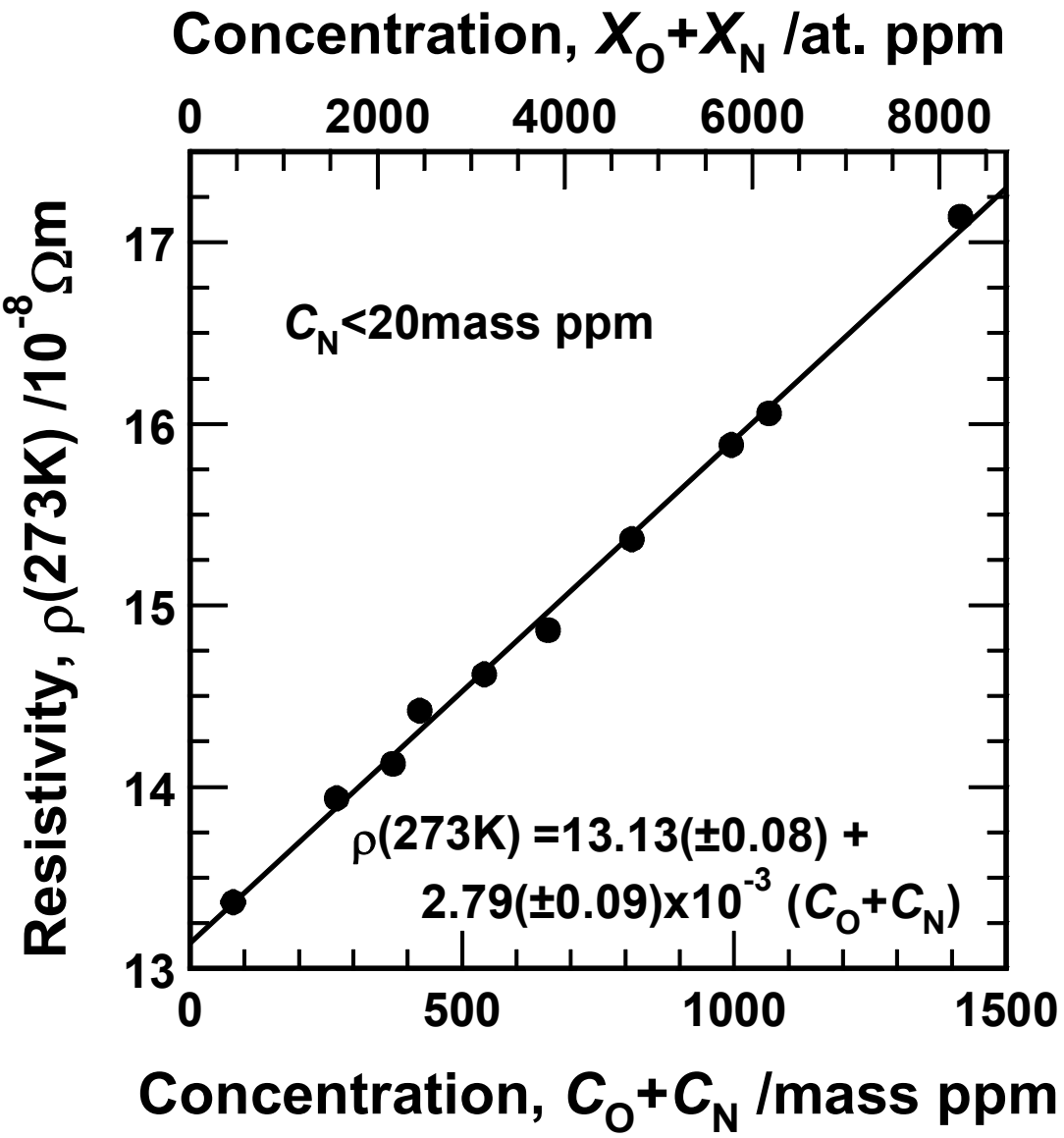

Fig. 6 Relationship between the sum of oxygen and nitrogen concentration, and the electrical resistivity at 273K.

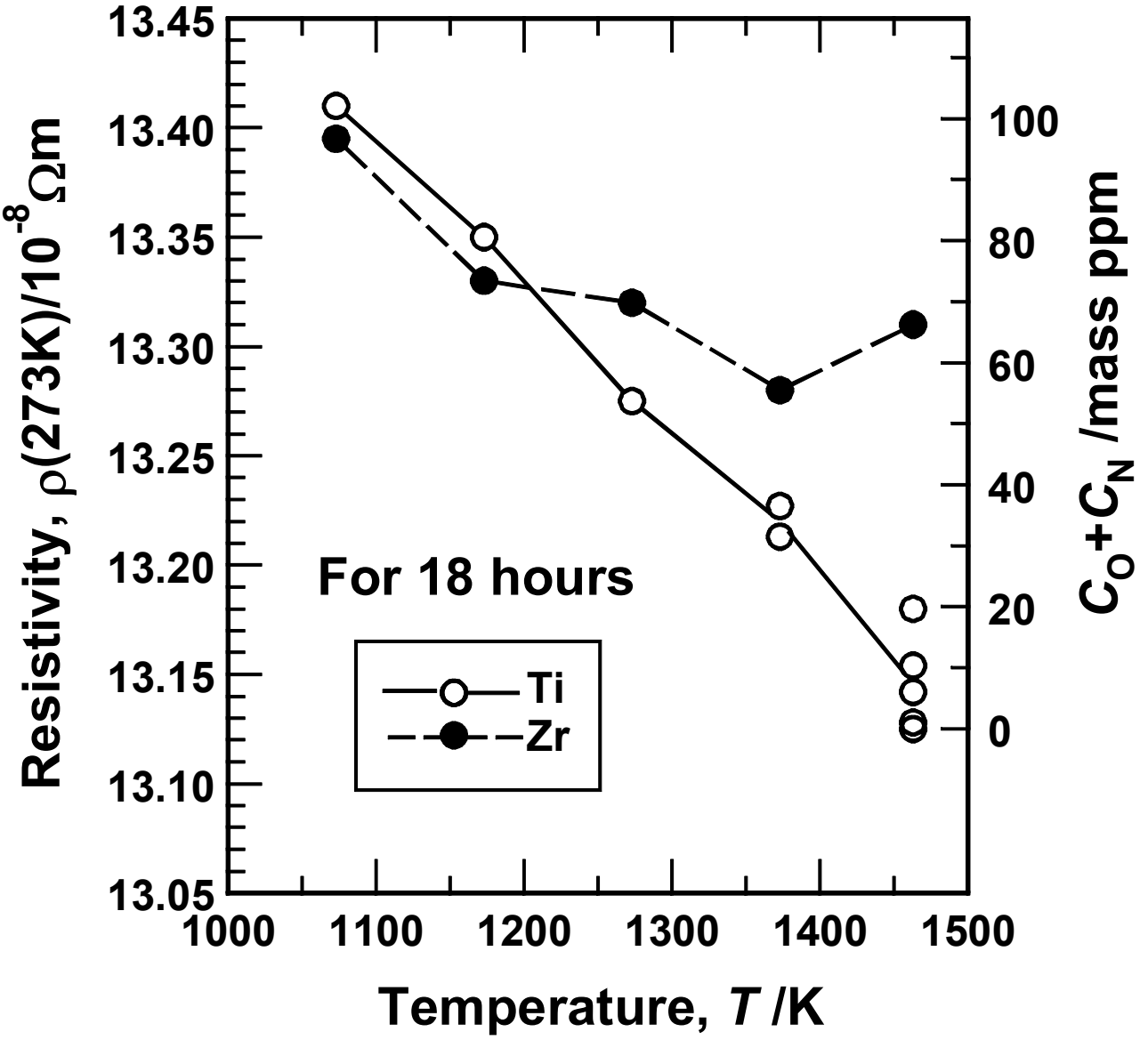

Fig. 7 Electrical resistivity at 273K of the samples annealed for 18 hours with Ti and Zr.

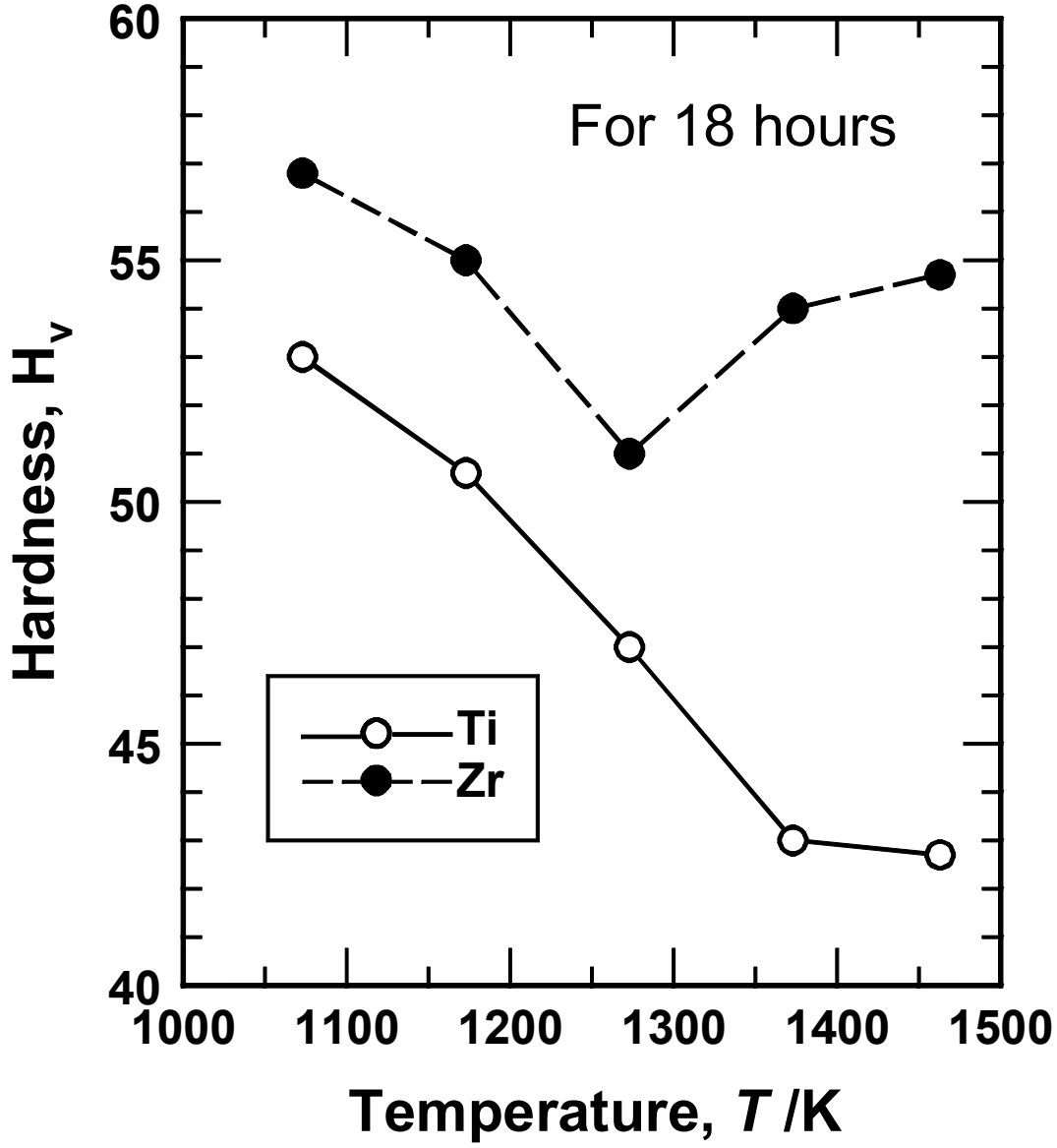

Fig. 8 Vickers' hardness of the samples annealed for 18 hours with Ti and Zr.

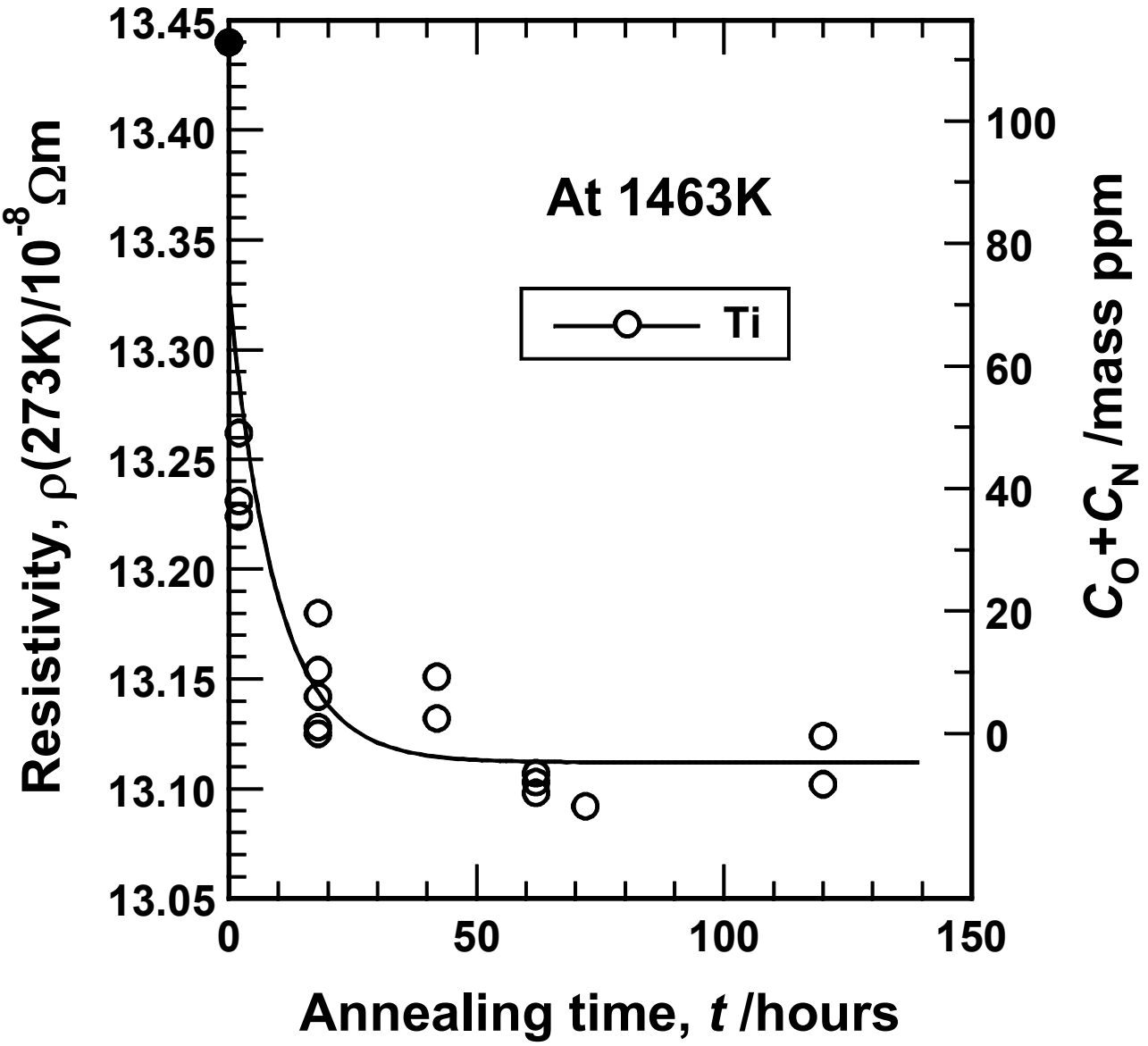

Fig. 9 Electrical resistivity at 273K of the samples annealed at 1463K with Ti.

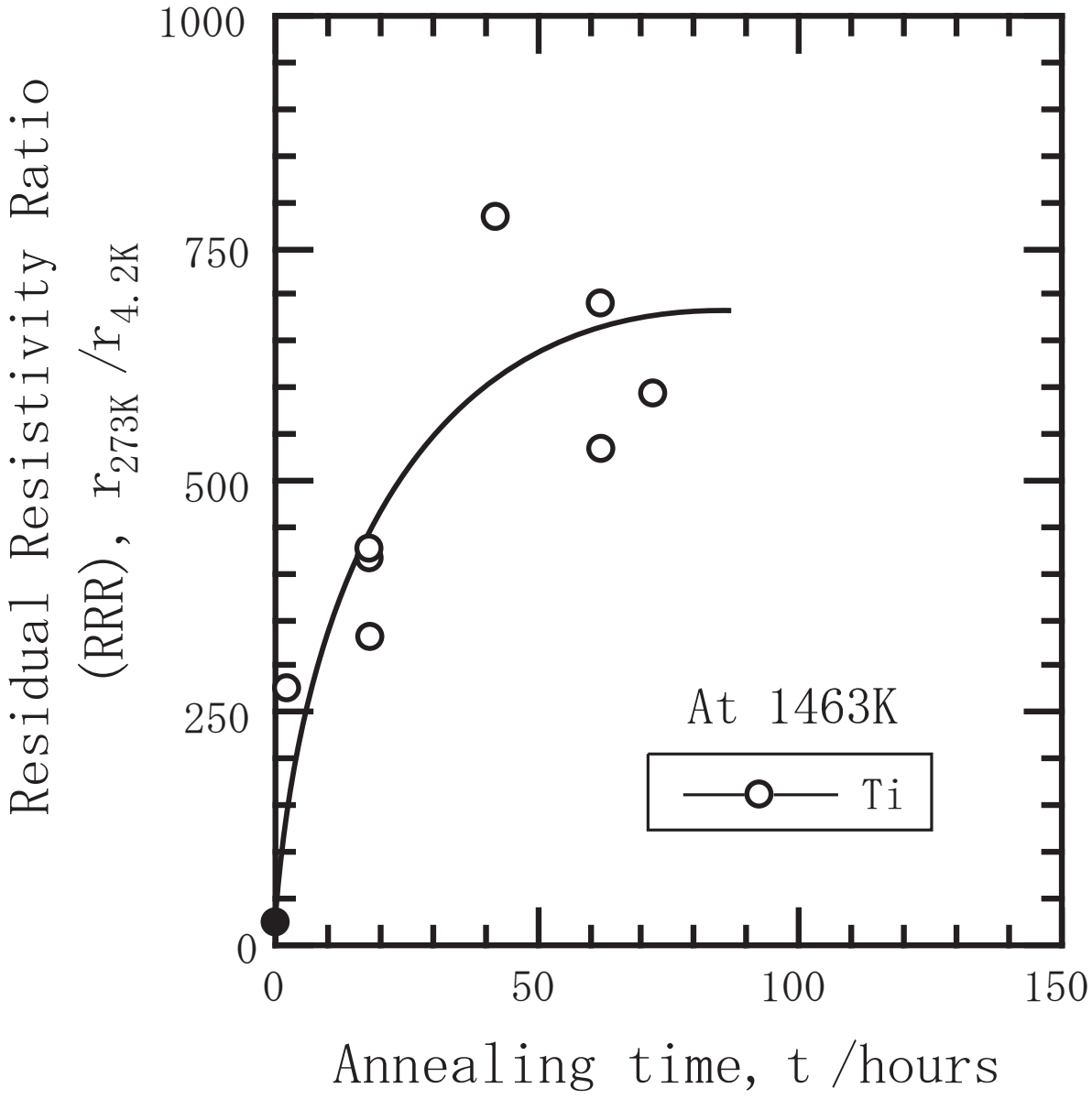

Fig. 10 Residual resistivity ratio of the samples annealed at 1463K with Ti.

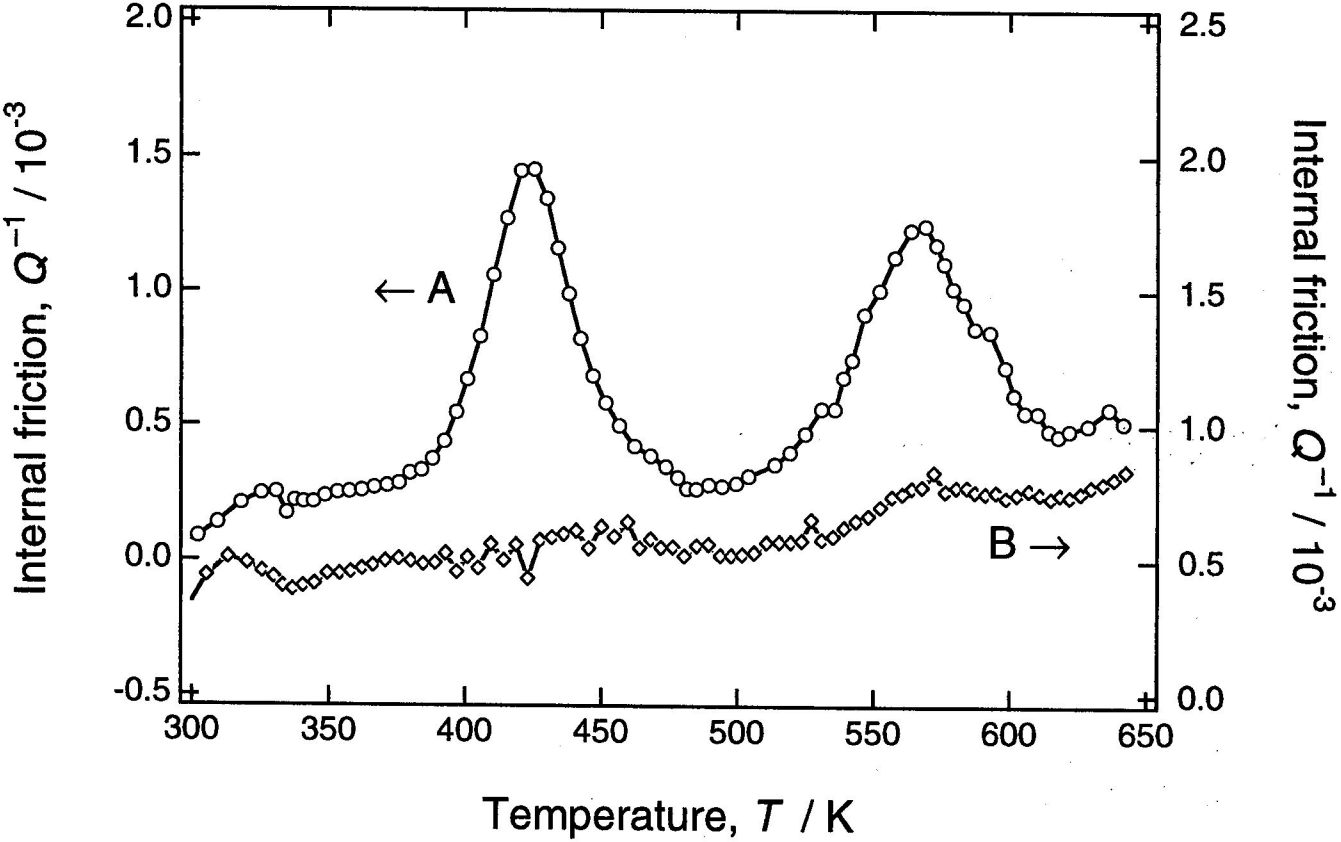

Fig. 11 Internal friction profiles of the sample (A) annealed without Ti, and of the sample (B) annealed with Ti, for 42 hours at 1463K.

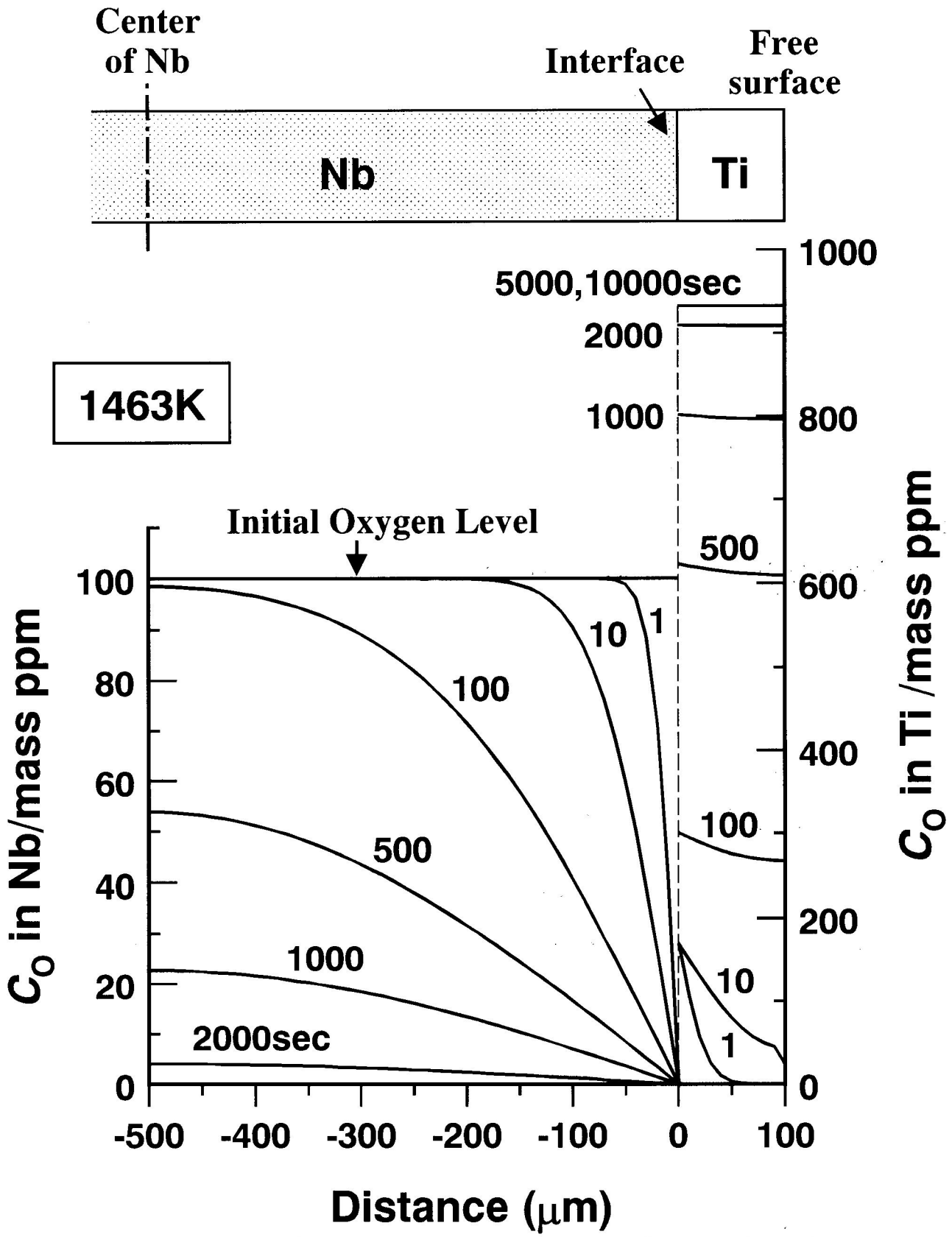

Fig. 12 Calculated oxygen profiles at 1463K, where the surfaces of 1mm thick niobium plate are coated by 100μm thick titanium layers.

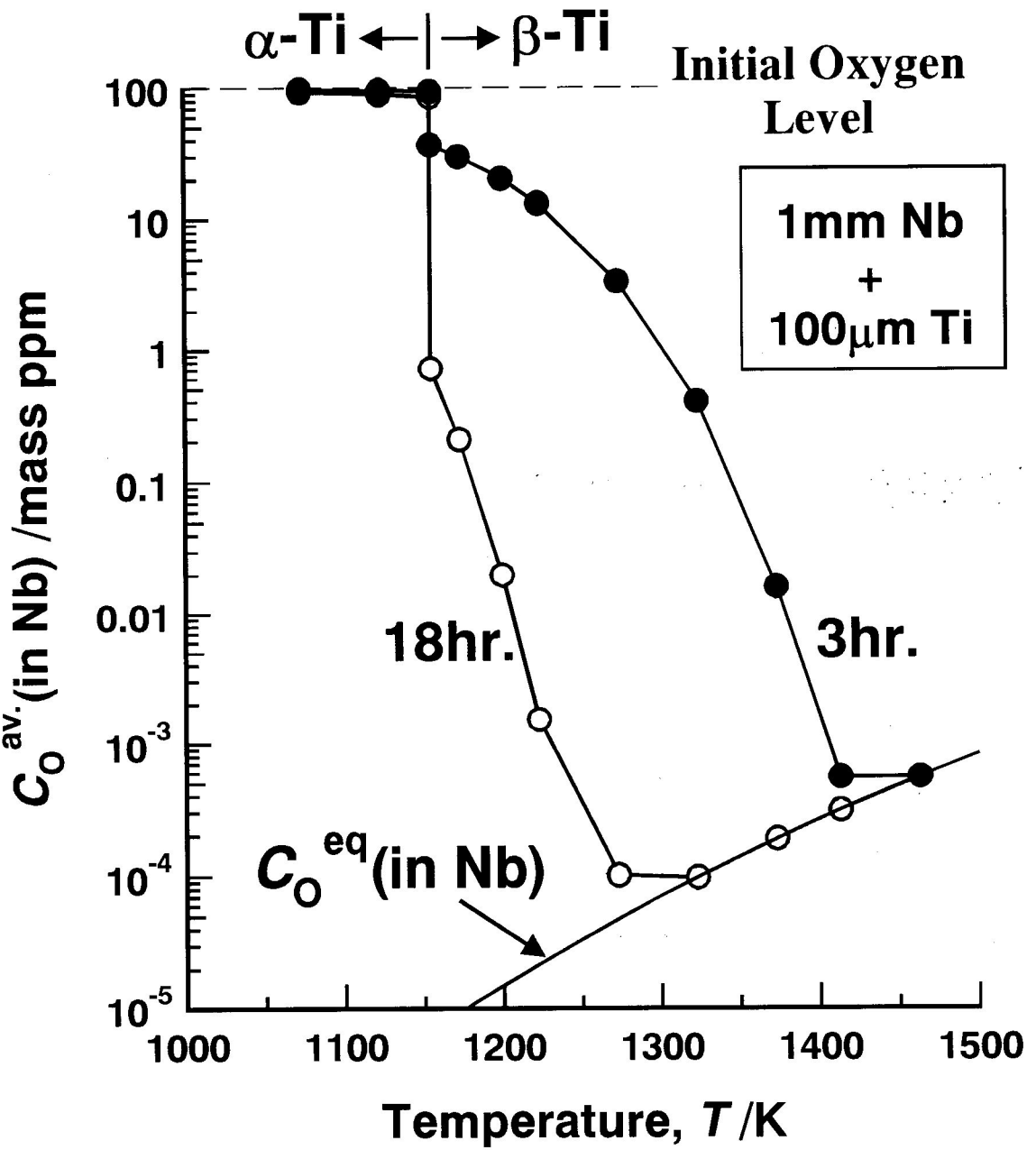

Fig. 13 Average oxygen concentration in 1mm thick niobium plate, whose surfaces are coated by 100μm thick titanium layers. Oxygen distributions were calculated for two annealing times, 3hours and 18hours.